

Response to reviewer 1

Dear Anonymous Reviewer 1,

we highly appreciate your feedback. It helped us to improve the manuscript. Below we comment on your suggestions in detail.

This paper reports measurements over a double ridge from a range of instruments (sonic anemometers on 100 m wind masts, Doppler lidars, etc.) made during the Perdigao field campaign in Portugal. The study focuses mostly on the occurrence of flow separation in the lee of the upwind hill, because of the importance for wind-power applications of the decrease of mean wind speed and increase of turbulence intensity that accompanies flow separation (and its effect on the downwind hill). The manuscript represents a substantial contribution to scientific progress, within the scope of ACP, being especially relevant due to the novel and comprehensive data gathered using state-of-the-art equipment. These data are processed and interpreted appropriately, although a number of improvements are possible (see below). The scientific approach, methodology and assumptions seem overall sound, and are described and discussed in an adequate, clear and balanced way, including allusions to previous work and use of references. Relevant results and conclusions supported by them are presented. The paper is concise, well-structured, clear, and well written. The title reflects the contents of the paper, and the abstract provides a good summary. The quality and number of figures and tables seems appropriate (for the content as it currently stands). The equations, symbols and units are properly defined and used. Although I will suggest some additions that require new calculations and possibly new figures, these should be straightforward to obtain from the existing data, so the paper is likely to require only minor revisions prior to publication.

General comment

Analysis of the collected data could be a bit more comprehensive, specifically regarding conditions under which flow separation is expected. These conditions may be estimated from simple, mostly linear, theories of flow over orography. Even ignoring boundary layer effects (which would complicate the picture considerably), flow separation can be viewed as an outcome of flow deceleration by the orography. Two paradigms may be considered in this problem. For neutral flow, nonlinearity may be quantified by (h/a) (the orography steepness), where h and a are typical height and width for the orography, and the flow perturbation scales as $U(h/a)$, where U is the incoming wind speed. For substantially stratified flow, on the other hand, nonlinearity is quantified by (Nh/U) , where N is the Brunt-Vaisala frequency of the incoming wind, and the horizontal flow perturbation scales as (Nh) . The authors consider Ri as a relevant parameter, but overlook the sensitivity of the flow to (Nh/U) , which would be equally easy to test and is even more basic (since it does not involve vertical derivatives of U). From the results presented in the paper, one gets the impression that neutral flow always causes flow separation (theoretically, this is predicted by (h/a) , which is fixed by the orography), but in statically stable conditions the important nonlinearity parameter becomes instead (Nh/U) , which might explain the absence of wave breaking detected when $Ri > 0$, i.e. $N^2 > 0$. With this conceptual framework, the fact that flow separation occurs for high wind speeds may be explained by the consequent smallness of (Nh/U) . The role currently played by Ri , in my view, is primarily distinguishing between unstable or neutral flows, on the one hand, and stable

flows, on the other, but it is not obvious that the wind shear effect contained in Ri has much relevance. This is one of the reasons why I suggest that the scaling with (Nh/U) be tested.

Thank you for outlining this theoretical background. We agree that we did not cover it well in the manuscript and included a new subsection (4.1.4) discussing our measurements in contrast to the results and findings of past experiments. More precisely, we present our result in the same non-dimensional framework as used in Baines (1995) Fig. 5.8 of h/A over Nh/U .

Specific comments

Page 1, lines 21-22: "flow acceleration and channeling effects, the formation of lee waves, and flow recirculation (Stull, 2012) which are not captured well by a linearized flow model". The word "well" is essential for this passage not to be grossly inaccurate. Linear models, with a structured atmosphere, are capable of predicting lee waves (Teixeira and Miranda, 2017), and can even give qualitative indications about flow channelling and recirculation (Teixeira, 2017). Linear models are almost the only way to obtain systematic scalings for the flow variables, and that should be recognized more in this passage.

Thanks for this comment. We meant to refer with the expression "*linearized flow model*" to software that is used in the wind farm planning process. We updated the manuscript, it reads now as follows: "A vast number of flow phenomena occur at sites with complex geometry (Rotach and Zardi, 2007), such as flow acceleration and channeling effects, the formation of lee waves, and flow recirculation (Stull, 2012) which are not captured well by frequently applied computer models (e.g. the Wind Atlas Analysis and Application Program, WAsP) in the wind farm planning process."

Page 4, line 5: "Range gates". It is not obvious to the reader what these mean exactly. Please add a brief description.

A description of the term has been added to the manuscript. The manuscript reads now as follows: "Range gates (time intervals used for determining the wind speed from the backscattered light. These time intervals corresponds to spatial intervals along the line-of-sight (LOS) for which the LOS wind speed is evaluated. They translate into a weighting function along the LOS which in this case has a full-width half-maximum of approximately 30 m.) were placed every 15 m, starting at a range of 100 m extending to 3000 m."

Page 6, lines 4-5: "[in order to calculate the Richardson number] we calculate the difference between the wind speed measured by the 100 m sonic and at the ground level, 0 m, where the wind speed is assumed to be zero". I assume that in this calculation and that of the vertical potential temperature gradient used to evaluate Ri the authors adopt linear interpolation in Eq. (1) (these details are not specified). The range of heights over which this calculation is performed is most likely in the surface layer. Since the profiles of both wind speed and potential temperature in that layer are logarithmic to a first approximation, it might be more accurate to determine Ri based on the logarithmic finite-difference approximation described by Arya (2001), Eq. (11.22). If this is not appropriate, please justify why.

In general, the estimation of the atmospheric stability is associated with high uncertainties, especially in complex terrain that we are investigating in a separate study in more detail. While a logarithmic approximation of the potential temperature profiles may be applicable under special conditions, our investigation of these profiles from the 100-m towers at Perdigao suggests that assumption is not reliable at this site (compare Stull (2003) Fig. 5.17) and we found a linear interpolation as used here may be more accurate. In our initial investigation, which included a comparison of several approaches for calculating the Richardson number, the Brunt-Vaisala frequency and Obukhov length, we found the Richardson number as a most reliable parameter to estimate the stability. (By “reliable”, we mean provided stability assessments consistent with time-of-day and did not lead to abrupt unreasonable transitions) Further, for the wind speed, a logarithmic approximation of the profile cannot be used since we decided to assume 0 m/s at 0 m height to minimize the effect of terrain-induced flow. An similar approach like ours has been used by Burns et al. (2011) and the reference has been added to the manuscript.

Figures 5 and 6: following my suggestions in the General Comment above, it would be probably useful to produce figures similar to these, but where Ri on the horizontal axis is replaced by (Nh/U) , or $U/(Nh)$. This should give some additional physical insight into the flow behaviour.

Thank you for the helpful suggestion. We have now included in the new section 4.1.4 a figure in which we present our observation under stratified conditions in the non-dimensional framework of h/A over Nh/U (see Figure 1 below).

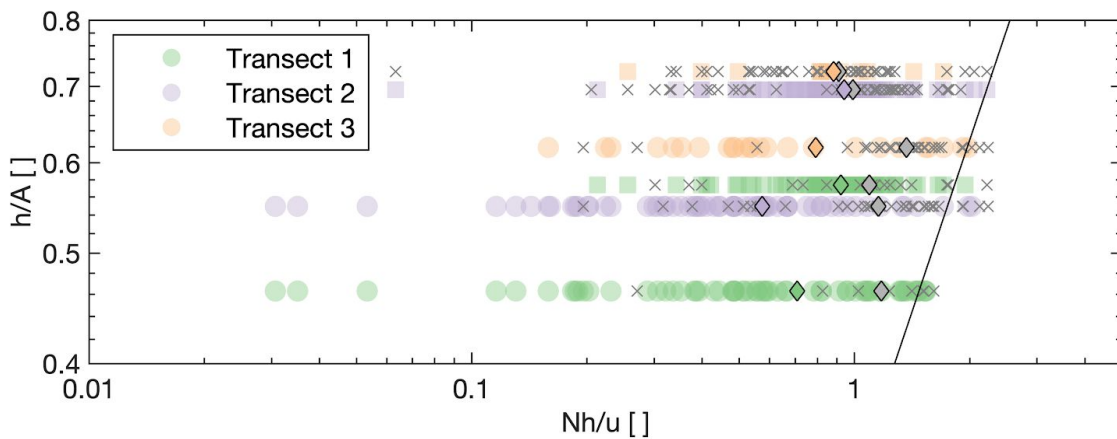


Figure 1: Observational periods with recirculation (colored markers) and without recirculation (gray cross marks) under stratified conditions as a function of mean lee-side slope (h/A) and Nh/u . The round markers refer to recirculation at the southwest ridge and the square markers to northeast ridge. The colored diamond markers show the mean value of Nh/u per transect during periods with recirculation and the gray markers the mean for periods without recirculation. The solid black line shows where $NA/u = \pi$.

Page 9, lines 2-3: "Recirculation is more likely to occur during unstable or neutral atmospheric conditions ($Ri < 0$) than for stable conditions ($Ri > 0$) for both SW and NE winds". The interpretation presented in my General Comment, along with plotting the data as a function of (Nh/U) , might be able to

shed some light as to why this happens. In terms of the behaviour with Ri , what appears to matter (see below) is the sign of N^2 , more than the detailed value of Ri . Perhaps this could be recognized and discussed.

Thanks for this comment. As mentioned above, we included section 4.1.4 which included a discussion of the mechanisms that are present under stratified conditions including a discussion of Nh/U .

Page 9, lines 13-18: Flow separation is discussed with relation to the height and steepness of the ridges. It is also noted that the southwest slope of the southwest ridge is steeper than the northeast slope of the northeast ridge. However, for flow separation in southwest flow what should be most important is the steepness of the northeast slope of the southwest ridge (because separation occurs downwind of obstacles) and for northeast flow the steepness of the southwest slope of the northeast ridge. The authors should check whether the steepnesses of these slopes are consistent with this physical interpretation of the results.

We appreciate this comment and updated the manuscript accordingly. The passage reads now as follows: “A possible explanation for this difference could be that the northeast face of the southwest ridge (the downwind face in southwesterly flow) has steep escarpments close to the ridge top and the average slope is slightly steeper compared to the southwest face of the northeast ridge (the downwind face in northeasterly flow). Both the higher steepness and the escarpments make flow separation more likely.”

Figure 8: the reverse flow speed is presented as a function of the upstream flow speed. As is consistent with my General Comment above, this tests a scaling for neutral flow, where the velocity perturbation scales as $u \sim U(h/a)$. This scaling is likely to be applicable, in Fig. 8, to the points that have $Ri < 0$ (i.e. $N^2 < 0$), because they will generate no orographic gravity waves. For points that have $Ri > 0$ (i.e. $N^2 > 0$), orographic gravity waves will occur, and the corresponding stratified scaling may apply, namely $u \sim (Nh)$. So, it would be interesting to produce a figure similar to Fig. 8, but with (Nh) in the horizontal axis. Perhaps a better collapse will be obtained for points with N^2 (although there are definitely many other processes going on, most prominently boundary layer effects). Even if this scaling with (Nh) does not work very well (for example, due to an insufficiently strong stratification), it is interesting to compare the two scalings.

Thanks for this comment. We tested the scaling with N^2 and it is definitely also interesting but doesn't give necessarily better insights than the use of the Richardson number. However, we decided to change Figure 8 to a dimensionless representation of reverse wind speed divided by the inflow wind speed over the Richardson number (Figure 2). Additionally, we generated Figure 3 that shows a comparison of the two scalings. This comparison of N^2 and Richardson number shows that both metrics agree well in the general classification of the different stability regimes.

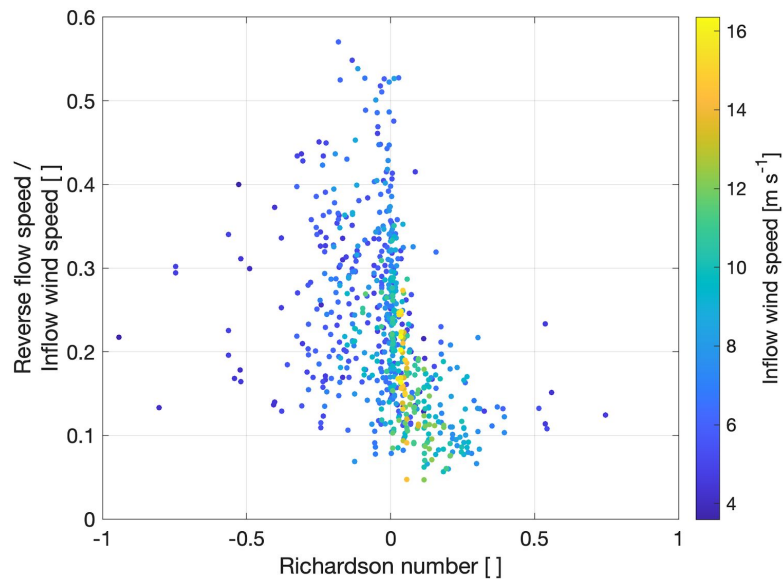


Figure 2: Maximum reverse flow speed divided by the inflow wind speed over the Richardson number. The color scaling shows the wind speed at the mast upstream.

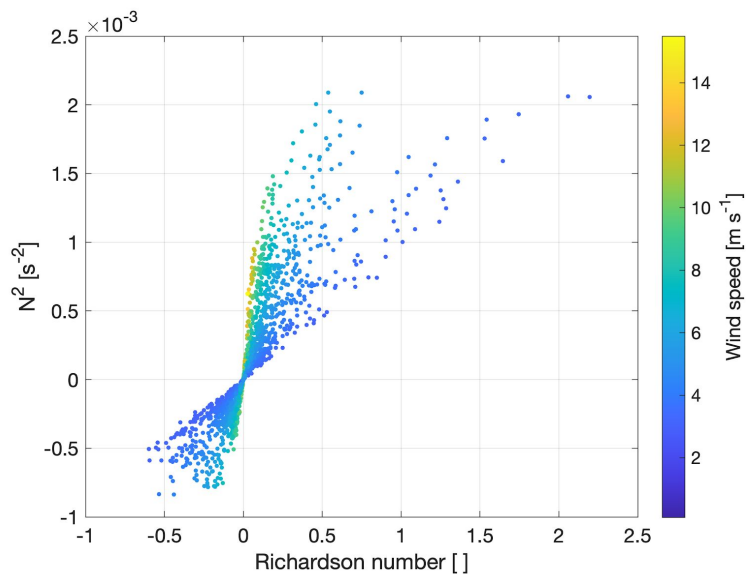


Figure 3: Comparison of N^2 and the Richardson number for wind speeds over 3 m/s. The color scaling shows the wind speed at the mast upstream.

Burns, S.P., Sun, J., Lenschow, D.H., Oncley, S.P., Stephens, B.B., Yi, C., Anderson, D.E., Hu, J. and Monson, R.K., 2011. Atmospheric stability effects on wind fields and scalar mixing within and just above a subalpine forest in sloping terrain. *Boundary-layer meteorology*, 138(2), pp.231-262.

Response to reviewer 2

Dear Anonymous Reviewer 2,

thank you for your critical feedback which helped us to improve this manuscript. Below we answer the specific comments in detail.

This manuscript uses Doppler lidar observations collected over the complex terrain of Perdigao to provide a qualitative description of recirculation on the lee side of the ridges. Recirculation was mostly observed under periods of neutral and unstable stratification during measurement campaign. Recirculation was also observed during stable conditions, albeit less frequently. Authors has made an effort to analyze the occurrence of recirculation along three transects and during southwesterly and northwesterly winds. The results of this paper could be useful for wind turbine siting in complex terrain, as well as to assess the performance of wind solvers qualitatively. Therefore, I support the publication of this manuscript after a revision that addresses the following issues.

1) Based on the content of the manuscript and the extent of the analysis, “Qualitative characterization of flow recirculation zones in complex terrain using multi-lidar measurements” would be a more adequate title for the investigation presented.

We appreciate this suggestion.

The request for the modification of the title was also raised by another anonymous reviewer. Accordingly, we changed the title of our manuscript to :

“Characterization of flow recirculation zones at the Perdigão site using multi-lidar measurements”
in order to reflect that this study was focused on the findings at the Perdigão site.

2) Vertical profiles of wind speed and direction during certain periods are needed to enable computational researchers to simulate the problem. These profiles should be extracted from multiple locations such from ridgetops and inside the recirculation zone and provided as new figures along with corresponding Richardson number.

The objective of this manuscript is not to provide model initiation data. All data sets measured during the Perdigão 2017 campaign are publicly available through dedicated Web portals of the University of Porto (<https://windsp.fe.up.pt/>) and NCAR/EOL (http://data.eol.ucar.edu/master_list/?project=PERDIGAO). Additionally, the DTU lidar measurement data is available under the following DOI: <https://doi.org/10.11583/DTU.7228544.v1>. We included the information on the data availability in the manuscript. This gives the opportunity to modelers to select initiation data to their needs, which is best suited for their specific application. We and other participants of the campaign are also very open to react on individual request to help with the selection of appropriate measurements.

3) Page 1 Line 15. The introduction to wind turbine siting is out of date (e.g. the cited reference is from 1989) and does not reflect the latest best practices. The discussion needs to be updated to reflect the current state of the art in this area.

The cited reference Troen and Petersen (1989) points to the European Wind Atlas that presents a methodology for wind turbine siting which is today except for small modification still widely used for site assessments. We decided to keep the reference to this work but updated the introduction with information on recent field campaigns (Lange et al., 2016) and modelling approaches (Silva Lopes et al., 2007, Chow and Street, 2009) with the aim to improve site assessments for the wind energy deployments.

4) Page 2 Line 5: Change “characterized” to “identified”. (i.e. flow recirculation can be identified . . .)

Thanks for this correction.

We assume that this comment refers page 2 line 3 and replaced “characterized” with “identified” in the manuscript.

5) Page 2 Line 5: Regarding authors’ discussion of the Kutter et al (2017). There is nothing unexpected about recirculation being “prevalent” during neutral or unstable conditions. If the hill or any obstruction is steep enough, the flow is expected to recirculate in the wake under those conditions. Therefore, instead of saying “Kutter et al. “find” recirculation prevalent during . . .” authors could say: “for instance, recirculation was prevalent during neutral and unstable atmospheric conditions during the observational study of Kutter et al.

We agree with the reviewer and changed the passage on page 2 line 8-9 as suggested.

6) Page 2 Line 10: Recirculation was intermittent in the Askervein experiment and the focus of Askervein was not to study recirculating flows. It would be better to refer to those studies as complex terrain studies as opposed to recirculation studies.

We agree that the main aspect of the Askervein was not to only measure recirculation. The passage has been updated.

7) There is no mention of the Bolund Hill experiment and related studies. Introduction section need to review those recent efforts since the Askervein case for completeness.

The introduction has been updated and includes now the Bolund hill experiment.

8) Figure 1: Please provide the dominant wind direction observed during the measurements and consider using a different marker for the wind turbine and refer to the Met Tower as Mast in the legend to be consistent with the text.

A wind rose showing the wind distribution measured at the northeast ridge has been added to figure 1. Moreover, the label and marker for the met mast have been changed.

9) Page 4, the paragraph section 3: Figure 1 should be redrawn to convey the information given in this paragraph about wind directions (i.e. the dominant wind directions should be overlaid on the figure.

A wind rose showing the wind distribution measured at the northeast ridge has been added to figure 1.

10) Page 5: Include a subscript G to emphasize gradient Richardson number in Equation 1

The subscript has been added.

11) *Figure 2: Make it larger for researchers who may need to digitize it. Create labels for SW Ridge and NE Ridge on the graph for sake of convenience for the readers.*

Thanks for recommending the use of labels for the two ridges, we included them in the figure 2. The figure is provided in a reasonable resolution, it can be easily scaled up on any computer for the purpose of digitization. Additionally, we included the coordinates of each transect as CSV files in the supplementary material. The terrain data is also part of the openly available datasets shared by the above mentioned institutions.

12) *Figure 4: Mark SW and NE ridges with labels on the terrain. Provide the gradient Richardson number for this 10 min period.*

Labels for the ridges also have been added for this figure and information about the gradient Richardson number is now provided in the caption.

13) *Figure 5: Increase the intervals in the x-axis so that the reader can approximately extract the Ri values without needing to digitize the graph. The bin width information in the caption is not helpful.*

We believe that the current number of bins presents the distribution well. We increased the size of the figure for better readability.

14) *Figure 5: It would be more useful to present Figure 5 per transect as done in Figure 6, but for the Ri number.*

We tested to present figure 5 also per wind direction and transect. The separation of the distributions into different transect did not add any additional insights. Accordingly, we decided to retain the current approach in presenting the results.

15) *Page 8 line 5: The features that are mentioned might play a role in the non- existence of recirculation, but the word “infer” is too strong in my opinion. Without a more detailed analysis, these features are suspects at best and insufficient to infer any flow behavior.*

We agree that the word “infer” might be too strong in this context, it has been replaced with “assume”.

16) *Page 9 line 5: Similar concern as in 5). The manuscript conveys the occurrence of recirculation in neutral and unstable conditions as if it is an unexpected feature. Re- circulation under those conditions for steep geometry or terrain are expected without any surprise. The more interesting finding would be recirculation under stable conditions, which is much more interesting. The discussion can be revised to describe observations and results that are expected and do not qualify as “findings”*

As suggested we made clear that flow recirculation can be expected for neutral and unstable conditions. The passage reads now as follows: “Recirculation is more likely to occur during unstable or neutral atmospheric conditions ($Ri \leq 0$) than for stable conditions ($Ri > 0$) for both SW and NE winds (Figure 5), as expect for flow over steep geometries such as the Perdigão ridges.”

17) *Authors can be more precise in their use of the term “stable conditions. Stable conditions need to be categorized as weakly, moderately and strongly stable based on the Ri number at hand, and authors can then compare against other studies that has similar conditions under that categorization.*

We are not aware of any other studies that present a categorization of stable conditions based the Richardson number in complex terrain. In general, a description of how the atmospheric stability can be described in complex terrain is missing. Existing methods to describe the atmospheric stability based on the Richardson number are validated for flat terrain and it is not straightforward to adopt a fine categorization for measurements in complex terrain. However, we included subsection 4.1.4 analysing our findings under stably stratified conditions in an non-dimensional framework which gives additional insights.

18) Authors are only relying on a generic categorization of stable conditions to explain the existence or non-existance of recirculation. Flow separation is highly dependent on the geometry. The current discussion fails to explain why recirculation exist or does not exist under stable conditions.

Subsection 4.1.4 which has been added to the reviewed version of the manuscript gives additional insights into the recirculation occurrences under stable conditions.

19) Conclusions: Provide the height for the 8 m/s wind speed.

We included the measurement height in the manuscript.

20) Conclusions: Typo in the last sentence. "Should be made".

Corrected.

Response to reviewer 3

Dear Anonymous Reviewer 3,

thank you for your extensive and constructive comments. Your feedback is highly appreciated. We comment on the suggestions in detail below.

General considerations

In this paper, the authors use a wonderful data set (from the Perdigão-2017 field campaign) to describe the ‘characteristics of flow recirculation zones in complex terrain’. Overall, the paper is quite well written and the provided material is useful to serve the purpose of the paper. However, some of the ‘ingredients’ of what is called an ‘algorithm’ to detect recirculation zones and some of the analysis tools need some clarification and reasoning (see the ‘minor comments’).

My major concern with this paper lies in the embedding of the obtained results in previous knowledge. The authors have decided to ‘wipe this away’ with a single comment (‘. . . which are not well captured by a linear flow model’, p1, l. 22) and therefore analyze the data with respect to each variable separately. First of all, linear theory is not all we know about flow behavior over topography, but more importantly, this decision leads to a ‘characterization’ that is entirely specific to the Perdigao site: all the given ‘numbers’ (e.g., in the conclusions: ‘recirculation is more likely for wind speed above 8 ms⁻¹’, p13, l.9) are not suitable to be transferred to any other site. In the end, the authors then (have to) conclude ‘Because assessment with multiple scanning lidars, as presented in this study, is yet not feasible for commercial projects, efforts should be [made] to account for recirculation in the flow models used for wind resource assessment’. While this is certainly a valid conclusion, in my view, additional generality could (easily) be obtained when at least discussing (using) some of the principles arising from previous knowledge. In this sense, the present ‘descriptive’ approach appears to be a missed opportunity. Clearly, a review cannot require from the authors to change their strategy of analysis – but I think the least that should be done is to comprehensively summarize the previous knowledge and discuss the ‘departures’ of the present site from the conditions, for which we have some theoretical understanding (major comment below). If the authors decide to keep their approach of analysis with respect to dimensional variables, the title should be changed (into something like ‘Characterization of flow recirculation zones at the Perdigao site using multi-lidar measurements’)

Major comment

Occurrence of recirculation behind a two-dimensional or three-dimensional obstacle has been widely investigated for stratified flow. Baines (1995) provides an excellent overview – see especially his Chapter 5. The characteristics of the mean flow behavior (over topography) are largely determined by the relative importance of stratification and advection in combination with the ‘obstacles’ dimensions (half-width, height) leading to an assessment of the flow characteristics in terms of non-dimensional parameters, Froude number (using the half-width of the ridge) or non-dimensional hill height (using the height).

At least for the stable cases (which are not abundant at the present location), therefore, the authors’ findings could be compared to previous knowledge with theoretical foundation. For example, Fig. 5.8 in Baines (1995) summarizes the occurrence of flow separation in a non-dimensional framework – and it would be extremely interesting to learn to what degree the re-circulation occurrence of the different

cross-sections at the present site correspond to those (mostly ideal) results. Certainly, on the basis of this previous knowledge, it would be much more conclusive to analyze the present data in a non-dimensional framework, rather than producing ‘thresholds’ for the mean wind and stability separately – and finding of course results that are surely consistent with this (larger mean wind speed favors separation, stronger stability hinders it) and then speculating that ‘These variations of recirculation occurrence may be related to the transects’ elevation profiles within the valley’, [p8, l.1]).

One of the relevant (and quite new) findings of the present study is certainly that re-circulation preferably occurs under unstable conditions (at the present site). This of course makes it more difficult to compare to previous knowledge for stratified flows. Even if the authors ‘rule out’ the value of linear theory (p1, l. 22), the Perdigao site is sufficiently ideal (and slopes may be steeper than desired for linear theory, but certainly not overly steep) that at least the consistency (in the trends) of the present results with the expectations from linear theory could be discussed. In fact, should be. The textbook of Kaimal and Finnigan (1994, their chapter 5) is an excellent source to start with – and Belcher and Hunt (1998) give a comprehensive overview of all the relevant resources. Again, stability is characterized in a non-dimensional framework using the terrain geometry (in this case the ‘inner-layer depth’, which could be determined from the present data) thus making the results more generally applicable.

The strongest ‘departure’ from applicability of previous knowledge is the ‘double ridge’ problem, i.e. the fact that at the Perdigao site not only one ridge is present but two – and those in a short enough distance so that they potentially influence the flow at each others’ location. There is less systematic knowledge available for this flow type with respect to recirculation zones – except for the quite specific case of rotor formation (which, of course, is also some sort of ‘recirculation zone’, but not immediately downstream of the ridge. See Grubisic et al. (2008) for some detail). Again, for the stable case, some information can be found in Baines’ book (but clearly less, and less theoretically founded). I think, this aspect may indeed be used in the discussion of the present results in view of potential departures from expectations for a single ridge.

Thank you for outlining this theoretical background! We agree that we did not cover it well in the manuscript and included a new subsection (4.1.4) discussing our measurements in contrast to the results and findings of past experiments. More precisely, we present our result in the same non-dimensional framework as used in Baines (1995) Fig. 5.8. Moreover, we changed the title of the manuscript to reflect that we concentrate our analysis on the observations at the Perdigão site, the title reads now as follows: “Characterization of flow recirculation zones at the Perdigão site using multi-lidar measurements”

Minor comments

P2/l. 28 Section 4 (not section)

Corrected.

Fig 1 caption: ‘Table 1’ (when using in conjunction with a number, please capitalize: Tab. 1,

Thanks for this remark. We corrected it throughout the manuscript.

Fig. 2 etc.). Throughout - many occurrences.

Corrected.

P2/l.10 many studies. . . : there are quite some others, e.g. discussed in Kaimal and Finnigan (1994).

The passage has been changed it reads now as follows:

“Many studies that are describing recirculation or in general flow over complex terrain rely on experimental data measured in the field. Probably the best known field experiment took place at the Askervein hill (Taylor and Teunissen, 1983). The measured data is heavily used to validate flow simulations such as linear models but also more sophisticated code using Reynolds averaged Navier-Stokes (RANS) methods (Silva Lopes et al., 2007) and large-eddy simulations (LES) as presented in Chow and Street (2009).”

P2/l.18 . . .the orography of the Perdigao site is more complex. . . : likely, the Perdigao site is as close to an ideal ‘two-dimensional ridge’ [more precisely, a valley between two two-dimensional ridges] as Askervein is to an ideal 3d hill. What is different is the dimensionality of the obstacle(s) and the slopes.

Thanks for this remark. We changed the manuscript according to the suggestion.

P3/l.7 SW and NE ridge, respectively.

“Respectively” has been added to the sentence.

P4, l.1 . . .for the exact directions: directions are not really provided in this table (of course, one could determine them by additionally using Fig. 1. . .).

The reference was supposed to point at Table 2 in which the exact orientation of the transects is stated.

P4/l.18 . . .due TO missing. . . However, until now we have only learned that two 100 m masts were used with sonics (p.3, l. 1) – now, all of a sudden, we have temperature measurements (which failed). Given the well-known problems with (absolute) accuracy of sonic temperature measurements, I do not hope that the authors have used the sonic temperatures to calculate Ri (also, it is hard to imagine that the sonic produces wind but no temperature. . .). It seems that the list of instruments (on p. 3) should be completed.

Thanks for this remark. The masts were also equipped with temperature sensors and we used this sensor data for the calculation of the Richardson number. We added the information to the manuscript it reads now as follows: “Starting in January 2017, a network of 50 measurement masts was deployed at the site, and over the next few months, 19 scanning Doppler lidars were added. For this study, we use the data from two 100-meter masts equipped with 3D ultrasonic anemometers (Gill WindMaster Pro) and temperature sensors (NCAR SHT75) located on the tops of the ridges as well as six scanning lidars (Figure 1 and, for exact positions, Table 1).”

Eq (1) In the equation, the authors write ‘T’, and after the equation they explain ‘T overbar’ (i.e., mean temperature). This must be consistent. However, the buoyancy term in the definition of the gradient Richardson number, in fact, should be defined with the potential temperature (not T), see, e.g., Stull (2012). While usually in Surface Layer micrometeorology, this is not really relevant, over the height of 100 m, this makes a difference.

Thanks for this remark we are using now consistently the potential temperature for our calculations.

P7/l. 8 'In overlap regions only measurements of the lidar further downwind are used'. I am not sure whether I understand this. What I understand then looking at Fig. 4a, the 'lidar further downwind' for the entire overlap region (which is the purple part) is the blue one, right? So, the second lidar is almost obsolete (only the really small part of the 'rim' is from this instrument. . .). This needs some reasoning. Also, looking at Fig. 4 suggests that the two lidars did not scan the same range (opening angle of the RHI). This should i) be mentioned where the scan strategy is introduced and ii) be motivated.

It is correct that the blue area corresponds to the scanning plane of the lidar further downstream. The "opening angles" or the range of elevations angles that is covered during one scan is for both lidars the same, namely 25° . The scans might appear different because the start angles, the lowest elevation angles, are different. The lidar on the SW ridge could start measuring under a lower angle since the position was more open and less restricted by obstacles.

It is not right to say the "second lidar is almost obsolete", it may appear so, but when we focus our view only at the area in between the two ridges, where we analyze the recirculation, it becomes obvious that the second lidar covers a substantial portion of this area which is not covered by the other lidar. The Figure 1 might help to illustrate the area proportions in between the ridges.

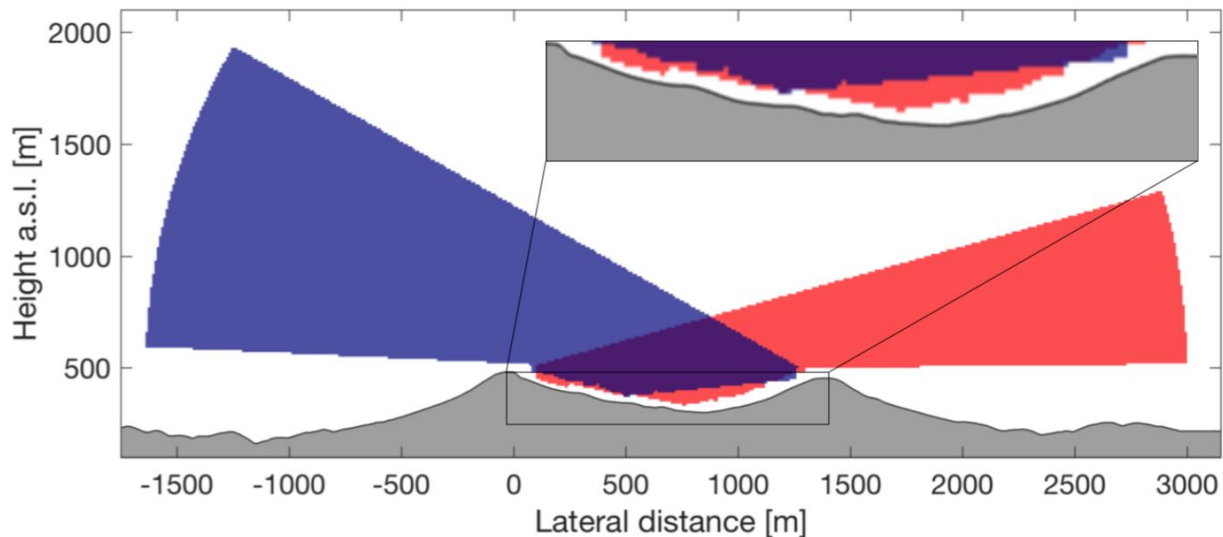


Figure 1: Schematic of the two RHI scans along a transect with magnification of the area in between the ridges.

P7/l.11 '. . .we do not attempt. . .': this seems to be at odds with l.7 (Cartesian coordinate systemwith the abscissa). The authors certainly need some rotation to do this, right? Does it mean that only one elevation angle for each RHI is used? I cannot see why this should be any easier to handle (and I cannot see what 'complex terrain' has to do with this). Can the authors please explain this procedure in some more consistency?

The two passages refer to independent steps. Line 7 refers to the procedure how measurements of the lidars are transferred to a common grid. L11 refers to the treatment of the LOS velocities. In flat terrain LOS velocities are often divided by the cosine of the elevation angle to get the horizontal wind component. We

cannot assume this for the Perdigão site. The second option would be to combine the measurements of the lidars to derive the vertical component which is not feasible since the elevation angles are too small to get correct results. The line has been rephrased and sounds now as follows:

“We do not attempt to combine LOS velocities measured by the lidars to get the true horizontal wind along the measurement transect, since the elevations angles are too small to measure the vertical component precisely. Moreover, the assumption of zero vertical wind speed, as often applied in flat terrain, is not valid in complex terrain.”

P9/l.15 ... is in general more ...

Corrected.

Fig 7 Unfortunately, the color coding in this figure is the opposite to that of Fig. 4.

The color coding has been changed, it is now identical to Figure 4.

Fig. 8 ‘reverse flow speed’: this should be specified (median, average over the recirculation zone, etc.).

We are using the maximum reverse flow speed, this has been added to the manuscript.

P11, l.11 ‘also influences [the] flow ...’: given the purely descriptive approach taken in this paper, in a case study one cannot conclude from one case that ‘the leeward recirculation zone and wake . . . decrease the mean wind speed. . .’. The wording has to be much more cautious (something like ‘for this case with a strong recirculation zone we observe a reduction in mean wind speed. . .’). Clearly, other cases with similar conditions but no recirculation zone would be needed to allow for a conclusion like ‘due to the recirculation zone wind speed is smaller and turbulence intensity larger’.

We chose a more careful wording for this passage and it reads now as follows: “For this case with a strong recirculation zone we observe a reduction in mean wind speed and increase the turbulence intensity at the northeast ridge.”

P12/eq (2) I am not convinced that the ratio of the median values is an extremely useful measure to demonstrate the slow-down (increase in turbulence intensity). This would be a (statistically) appropriate measure, if wind speed were normally distributed (but often it is not). Is there any reason not to use a proper ‘delta’ $(U_{ds} - U_{us})/U_{us}$ (‘ds’=downstream, ‘us’=upstream), and average over all cases? If the sign of this measure were significantly different from zero (and significance can be tested. . .) – and even ‘more negative’ for recirculation occurrence than for no occurrence, this would be a strong indication that there is a reduction in mean speed (increase in intensity) due to the recirculation zone.

We agree that it is more clear and intuitive to use a delta as suggested. Table 4 has been completely updated to make the comparison of mean turbulence intensity and mean wind speed between up- and downwind ridges during periods with and without recirculation more clear.

Tab. 4 If the ‘delta’s are defined as in eq (2), the given information is not in % (if the median ratio for ‘recirc’ is 0.42, say, and that for ‘no recirc’ is 0.50, the indicated difference amounts to -0.08 – and not even multiplying with 100 makes this to be an 8.2% reduction. . .). Definition of those ‘delta’s and their use should be made clear and the wording adjusted.

See comment above.

P13/l.4 'Algorithms are developed...': In fact, it is only one – and it is not really an algorithm, but rather a straight forward ad hoc procedure.

We corrected this line and referring no to the procedure of detection recirculation zones as method instead of algorithm. Additionally, we added a flow diagram of the detection process (Figure 2) to make the process more clear to the reader.

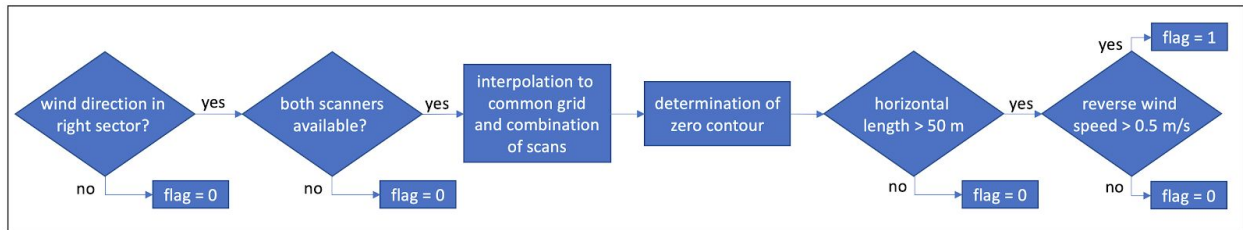


Figure 2: Flow diagram of the recirculation zone detection process.

P13/l.21 should be made

Corrected.

Characterization of flow recirculation zones ~~in complex terrain at~~ the Perdigão site using multi-lidar measurements

Robert Menke¹, Nikola Vasiljević¹, Jakob Mann¹, and Julie K. Lundquist^{2,3}

¹Technical University of Denmark - DTU Wind Energy, Fredriksborgvej 399, Building 118, 4000 Roskilde, Denmark

²Department of Atmospheric and Oceanic Sciences, University of Colorado, Boulder, Colorado, USA

³National Renewable Energy Laboratory, Golden, Colorado, USA

Correspondence: Robert Menke (rmen@dtu.dk)

Abstract. Because flow recirculation can generate significant amounts of turbulence, it can impact the success of wind energy projects. This study uses unique Doppler lidar observations to quantify occurrences of flow recirculation on lee sides of ridges. An extensive dataset of observations of flow over complex terrain is available from the Perdigão-2017 field campaign over a period of three months. The campaign site was selected because of the unique terrain feature of two nearly parallel ridges with a valley-to-ridge-top height difference of about 200 m and a ridge-to-ridge distance of 1.4 km.

Six scanning Doppler lidars probed the flow field in several vertical planes orthogonal to the ridges using range-height-indicator scans. With this lidar setup, we achieved vertical scans of the recirculation zone at three positions along two parallel ridges. We construct a method to identify flow recirculation zones in the scans, as well as define characteristics of these zones. According to our data analysis, flow recirculation, with reverse flow wind speeds greater than 0.5 m s^{-1} , occurs over 50% of the time when the wind direction is perpendicular to the direction of the ridges. Atmospheric conditions, such as atmospheric stability and wind speed, affect the occurrence of flow recirculation. Flow recirculation occurs more frequently during periods with wind speeds above 8 m s^{-1} . Recirculation within the valley affects the mean wind and turbulence fields at turbine heights on the downwind ridge in magnitudes significant for wind resource assessment.

1 Introduction

Traditional wind turbine siting relies on wind measurements from a single mast or a small number of masts deployed at the site of interest. These measurements are extrapolated over the entire site using a linearized flow model to provide a general assessment of wind resources (Troen and Petersen, 1989). This method proved suitable for flat terrain sites, gently sloping terrains and offshore where the flow is close to being homogeneous. In complex terrain, however, where wind fields are strongly affected by the topography and roughness changes, the uncertainties of wind resource estimations are increased because models struggle to predict flow under these conditions, despite of continues advancement of flow models. A vast number of flow phenomena occur at sites with complex geometry (Rotach and Zardi, 2007), such as flow acceleration and channeling effects, the formation of lee waves, and flow recirculation (Stull, 2012) which are not captured well by ~~a linearized flow model~~. frequently applied computer models (e.g. the Wind Atlas Analysis and Application Program, WASP) in the wind farm planning process. These effects have high spatial and temporal variability and are thus difficult to investigate with sparse measurements. However, these

phenomena can induce high loads on wind turbines which will decrease turbine lifetime (Sathe et al., 2013), and therefore such effects must be characterized and understood in order to be able to predict them.

In this study, we investigate flow recirculation occurring in the lee of ~~a hill or a ridge~~ ridges. Flow recirculation can be ~~characterized~~ identified by flow moving reversely to the prevailing flow direction. In this region both turbulence and wind shear are increased (Stull, 2012). Recirculation occurs behind abrupt drops in terrain elevation such as cliffs, but also in the lee of gentle slopes of a certain steepness (Wood, 1995; Xu and Yi, 2013; Kutter et al., 2017). In addition, small terrain features (Lange et al., 2017) and the presence of forest canopy (Sogachev et al., 2004; Finnigan and Belcher, 2004) can modify the occurrence of recirculation drastically. Furthermore, the stratification of the atmosphere influences the occurrence of recirculation; ~~Kutter et al. (2017) find recirculation for instance, recirculation was~~ prevalent during neutral or and unstable atmospheric conditions in their observational study—during the observational study of Kutter et al. (2017). The length of flow separation zones is mainly dependent on the hill shape and the surface roughness. Increasing downwind slopes and larger roughness is causing longer separation zones. In Kaimal and Finnigan (1994) a usual extend of the separation zones for naturally shaped hills of two to three times the hill height is stated.

Many studies ~~of recirculation rely on data collected during the Askervein experiment (Taylor and Teunissen, 1983; Silva Lopes et al., 2007)~~ The Askervein data set provides measurements in heights from 10 to 50 m along a transect crossing an isolated, gently sloping hill with average slope angles of 11° in Scotland. Consequently, the spatial resolution and the ability to observe flow above 50 m was absent that are describing recirculation or in general flow over complex terrain rely on experimental data measured in the field. Probably the best known field experiment took place at the Askervein hill (Taylor and Teunissen, 1983). The measured data is heavily used to validate flow simulations such as linear models but also more sophisticated code using Reynolds averaged Navier-Stokes (RANS) methods (Silva Lopes et al., 2007) and large-eddy simulations (LES) as presented in Chow and Street (2009). Another, more recent field experiment is the Bolund hill campaign which took place in 2007-2008. A blind test of different microscale flow models for the Bolund case revealed major uncertainties in predicting the influence of the Bolund escarpment on the flow field. The experiment also demonstrated the strength of lidars, in their case continuous-wave Doppler lidars, to measure the influence of the Bolund escarpment on the flow field (Lange et al., 2016). Here, we investigate measurements from the Perdigão 2017 campaign where, in addition to sonic anemometers on 100-m high masts, pulsed Doppler lidars observed the flow over the two parallel ridges. To surpass the capabilities of point measurements from networks of ~~towers~~ masts, Doppler lidars have, not only in the Bolund campaign, proved capable of measuring flow phenomena such as wind turbine and wind farm wakes (Käsler et al., 2010; Iungo et al., 2013; Aitken et al., 2014; Menke et al., 2018) and the effect of roughness changes on wind fields in different heights and nearshore flows (Mann et al., 2017). In addition to the advancements in the measurement technology, the orography of the Perdigão site ~~is more complex than at Askervein. Slope angles at the~~ can be approximated by two two-dimensional ridges as the Askervein's orography with an three-dimensional hill of about half the height of the Perdigão site are higher with average slope angles of more than 23° , and the double ridge adds additional complexity ridges.

The present work uses multi-lidar measurements to observe and classify recirculation that occurs in the lee of ridges at Perdigão. The flow field is measured by six scanning lidars at three different transects across the ridges. The scans cover

the entire recirculation zone, enabling us to characterize the dimensions of recirculation zones and to investigate their spatial variability along the ridges. Moreover, we relate these recirculation zones to resulting changes in turbulence and wind shear measured by sonic anemometers on measurement masts at potential wind turbine sites downwind of recirculation zones. The measurement campaign, Perdigão 2017 (Mann et al., 2017; Fernando et al., 2018) is presented in Section 2 of this manuscript.

5 In ~~section~~[Section 3](#), we describe how the lidar measurements are used to detect recirculation zones. The occurrences of recirculation at the Perdigão site are analyzed with respect to mean wind speed and atmospheric stability in ~~section~~[Section 4](#). In addition, we assess the impact of recirculation at potential turbine sites in this section. Conclusions are given in the last section.

2 Field campaign overview and measurement data

10 The experiment is part of a series of measurement campaigns within the New European Wind Atlas with the objective to provide an extensive dataset of high-quality measurements of flow over complex terrain (Mann et al., 2017). Starting in January 2017, a network of 50 measurement masts was deployed at the site, and over the next few months, 19 scanning Doppler lidars were added. For this study, we use the data from two 100-meter masts equipped with 3D ultrasonic anemometers (Gill WindMaster Pro) [and temperature sensors \(NCAR SHT75\)](#) located on the tops of the ridges as well as six scanning lidars (Figure 1 and, 15 for exact positions, Table 1). Here, we focus on the period of 68 days from April 8 to June 14 during which long-range WindScanners and masts operated in parallel.

2.1 Measurement site

The measurement site, located in central Portugal near the Spanish border, was selected because of the unique terrain feature of two nearly parallel ridges with a valley-to-ridge-top elevation difference of about 200 m and a ridge-to-ridge distance of 1.4 km 20 (Figure 1). The ridges run from the northwest to the southeast and are hereafter referred to as SW and NE ridge, [respectively](#). The terrain roughness is characterized by a patchy vegetation of pine and eucalyptus trees with heights of up to 15 m. A detailed site description can be found in Vasiljević et al. (2017).

2.2 WindScanner measurements

We deployed six long-range WindScanners, scanning-Doppler lidars (Vasiljevic et al., 2016), on top of the ridges at the 25 Perdigão site. All scanners performed range-height-indicator (RHI) scans along three transects which are almost perpendicular to the ridges. The transects are orientated along the SW-NE direction (Figure 1, see Table [1-2](#) for the exact directions). The scans with a maximal range of 3 km covered the area within the valley. Outside the valley, the scans covered areas to a maximum range of 3 km and up to 1600 m above ground level. Elevation profiles along the transects are shown in Figure 2. We measured continuously during the upwards movement of the scanners with an averaging elevation angle of 0.75° over a range 30 of 25° . Range gates ([time intervals used for determining the wind speed from the back-scattered light. These time intervals corresponds to spatial intervals along the line-of-sight \(LOS\) for which the LOS wind speed is evaluated. They translate into](#)

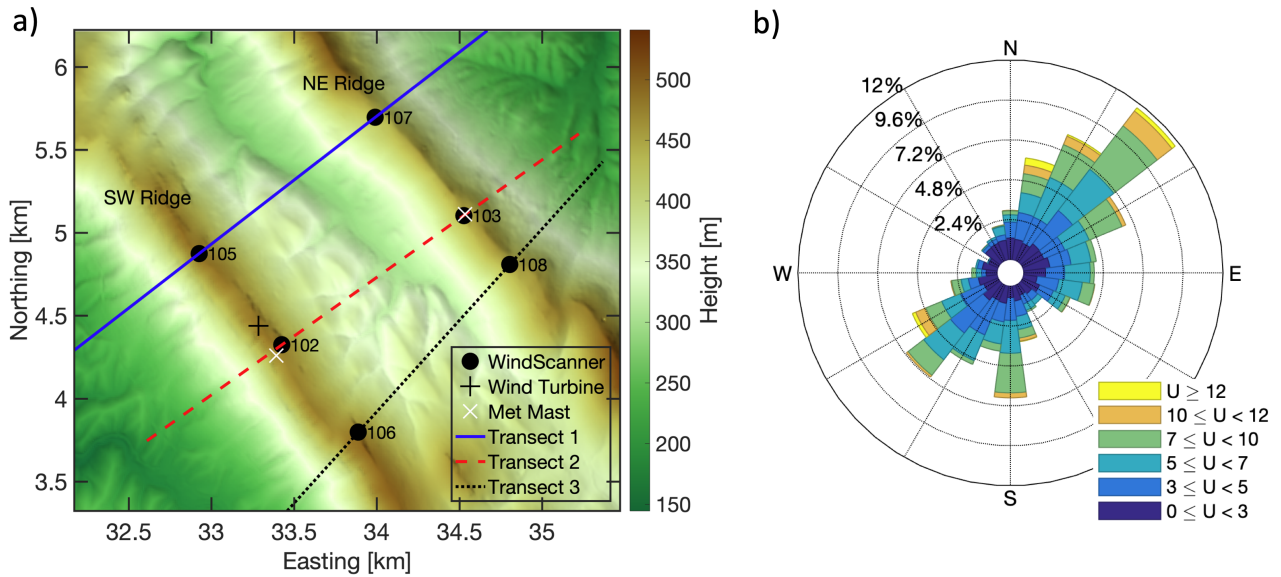


Figure 1. a) Elevation map of the Perdigão site. Measurement transects are indicated by the solid blue (Transect 1), dashed red (Transect 2) and dotted black (Transect 3) lines. Black disks: WindScanner positions; Numbers: WindScanner station number as in [table-Table 1](#); Black \times : wind turbine position; White X's: position of measurement masts used in this investigation. PT-TM06/ETRS89 coordinate system, height above sea level. b) [Distribution of 30-minute averaged wind measurements taken by the 100 m anemometer on the mast located on the northeast ridge over the period from April 1 to June 15, 2017. Measurements in \$\text{m s}^{-1}\$.](#)

Table 1. Positions of instruments used in this study. Easting and northing in PT-TM06 / ETRS89 coordinate system and elevation above sea level. Elevation of the [towers-masts](#) (first two rows) refers to the [tower-mast](#) base and elevation of the WindScanners (remaining rows) refers to the scanner head position.

Station Number	Station Acronym	Easting [m]	Northing [m]	Elevation [m]
20	20/tse04	33392.7	4259.6	473.0
29	29/tse13	34533.6	5112.0	452.9
105	LRWS #5(DTU)	32926.5	4874.3	485.9
107	LRWS #7(DTU)	33990.6	5695.3	437.1
102	LRWS #2(DTU)	33426.2	4324.1	480.3
103	LRWS #3(DTU)	34526.3	5103.5	452.3
106	LRWS #6(DTU)	33888.7	3798.0	486.3
108	LRWS #8(DTU)	34804.6	4807.9	452.8

[a weighting function along the LOS which in this case has a full-width half-maximum of approximately 30 m.](#)) were placed every 15 m, starting at a range of 100 m extending to 3000 m. The effective probe length of the scans was 35 m along the laser

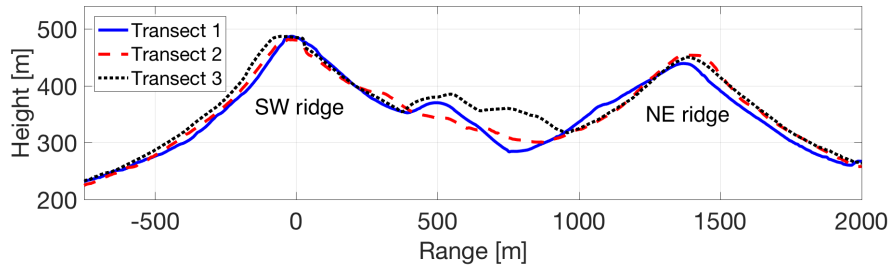


Figure 2. Elevation profiles of measurement transects. The transect colors correspond to [figure Figure 1](#). The vertical scale is exaggerated by a factor of two. The origin (range = 0) refers to the position of WindScanner 105, 102 and 106 for transect 1, 2 and 3, respectively. [The coordinates of the transects are available as CSV files in the supplementary material.](#)

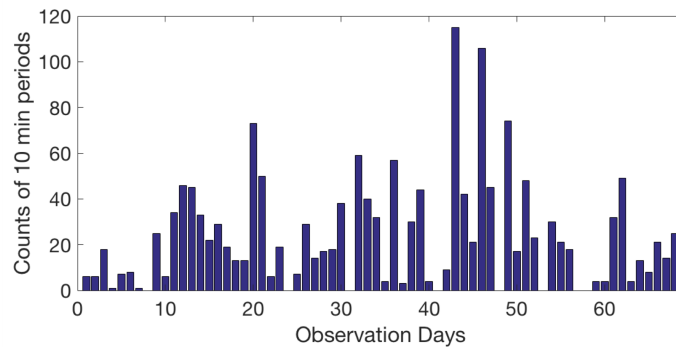


Figure 3. Distribution of the 1613 available 10-minute periods with wind directions perpendicular to the ridges ($214^\circ - 254^\circ$ and $34^\circ - 74^\circ$). The observational period lasted for 68 days starting on 2017/04/08 and ending on 2017/06/14. The intensive observation period of the campaign started on day 24 (2017/05/01). [The availability data can be found the in the supplementary material.](#)

light propagation path. The RHI scans were carried out twice per hour for 10 minutes by all lidars. During one 10-minute period, 23 scans were performed; a single scan took about 26 seconds to complete. We averaged the data over each 10-minute period, after filtering the data by the carrier-to-noise-ratio ($CNR < -24$ dB) and removing hard target influences. To ensure that the pointing accuracy of minimum 0.05° is maintained during the entire measurement period, the WindScanner's leveling was checked and the known hard targets were mapped consistently through the measurement campaign (Vasiljević et al., 2017).

For the analysis, we selected periods within two 40° wind direction sectors centered at a line perpendicular to the ridge ($214^\circ - 254^\circ$ and $34^\circ - 74^\circ$). The direction is measured by the 100-m sonic anemometer on the mast located on the southwest ridge. In total, 1619 10-minute periods of measurements are available for the analysis in these sectors (Figure 3).

Table 2. Parameters describing the measurement transects. Peak height gives the highest points at the southwest (SW) and northeast (NE) ridge, respectively. The average terrain elevation is measured along the transects in between the peaks. The maximum height of the ridges relative to the terrain height at the transect before and after the ridges is given by h_{SW} and h_{NE} . A_{SW} and A_{NE} is the half-width at half-height of the faces inside the valley.

Transect	Transect	Orientation	Orientation	Peak height	Peak height	Average	Lowest point	Peak-to-peak	h_{SW}	A_{SW}	h_{NE}
			[deg]	SW ridge [m]	NE ridge [m]	height [m]	in valley [m]	distance [m]	[m]	[m]	[m]
1	1		52.3	487.1	439.3	369.7	283.5	1388.0	278.6	601.6	230.0
2	2		54.7	481.6	453.8	369.2	300.3	1425.6	268.4	488.6	240.0
3	3		42.2	487.0	450.7	384.2	317.2	1435.8	237.3	383.3	201.0

3 Methods

3.1 Atmospheric stability

To define atmospheric stability, we calculated the gradient Richardson number at the mast located on the Northeast ridge (figure Figure 1). The SW ridge mast could not be used due missing temperature measurements for a major part of the observational 5 periods. The gradient Richardson number is defined as in Stull (2012) :

$$Ri_G = \frac{\frac{g}{T} \frac{\partial \bar{\Theta}}{\partial z}}{\left[\left(\frac{\partial \bar{U}}{\partial z} \right)^2 + \left(\frac{\partial \bar{V}}{\partial z} \right)^2 \right]} \frac{\frac{g}{\bar{\Theta}} \frac{\partial \bar{\Theta}}{\partial z}}{\left[\left(\frac{\partial \bar{u}}{\partial z} \right)^2 + \left(\frac{\partial \bar{v}}{\partial z} \right)^2 \right]} \quad (1)$$

where \bar{T} is the mean temperature measured at 100 m, $\partial \bar{\Theta}$ the potential temperature difference between 10 m and 100 m, $g = 9.81 \text{ m s}^{-2}$ is the gravitational acceleration, and U and V u and v are the two horizontal components of the mean wind vector. The potential temperature is approximated by $\bar{\Theta} \approx T + (g/C_p) \cdot z$ where $g/C_p = 0.0098 \text{ Km}^{-1}$ (Stull, 2012). In order to reduce 10 the effect of terrain-induced flow on the stability estimates, we calculate the difference between the wind speed measured by the 100 m sonic and at ground level, 0 m, where the wind speed is assumed to be zero. A similar approach has been used by Burns et al. (2011). All calculations are based on 30-minute averages. In total we could assess the atmospheric stability for 82% of the 10-minute periods due to missing temperature data from the meteorological tower mast.

Moreover, the Brunt-Väisälä frequency which is defined as:

$$N = \sqrt{\frac{g}{\bar{\Theta}} \frac{\partial \bar{\Theta}}{\partial z}} \quad (2)$$

is estimated from the mast measurements for stably stratified conditions. We use again the potential temperature difference between the 10 m and 100 m levels at the mast on the northeast ridge.

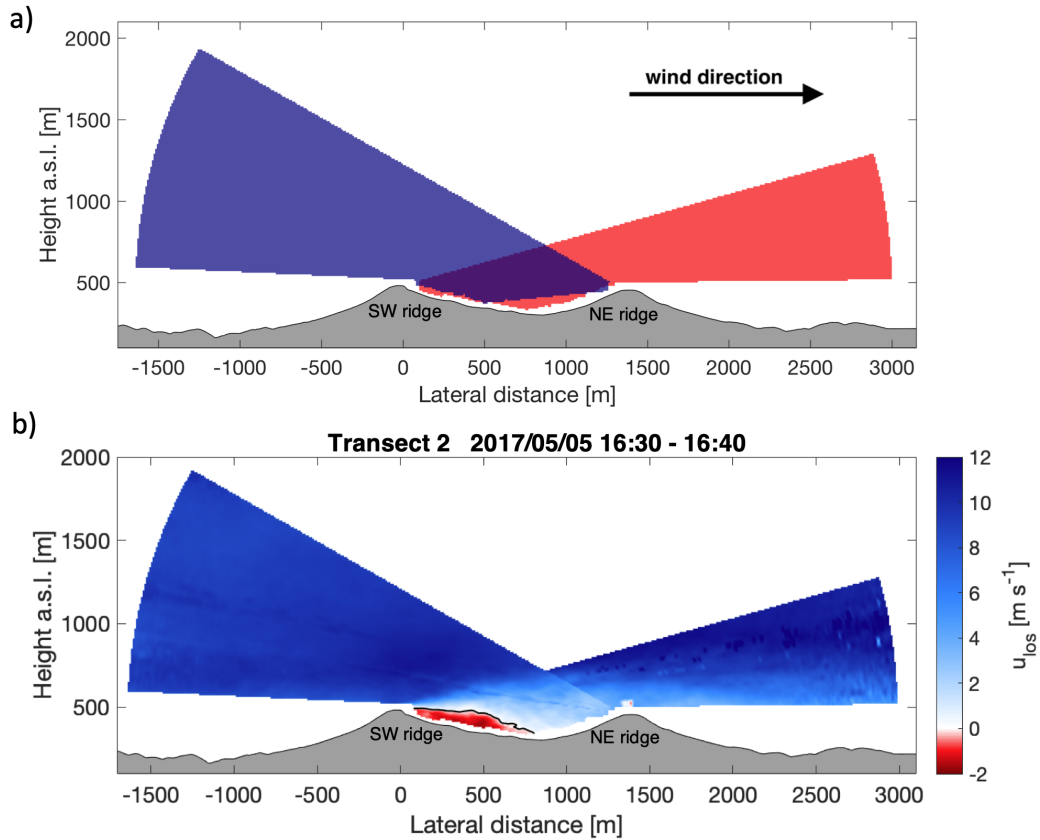


Figure 4. Detection of recirculation zones at the second transect (lateral distance = 0 is the position of WindScanner 102), view from the southeast. a) Schematic of the overlay of the two RHI scans at the transect. Blue and red areas are corresponding to the RHI scans and the grey area shows the terrain. b) Lidar measurements along the transect and detected recirculation zone for one 10-min period [with \$Ri_G \equiv 0.016\$](#) . Positive LOS velocities indicate flow towards the northeast (from left to right in the plot). The terrain is plotted in grey and the contour line defining the recirculation zone is plotted in black inside the velocity field. Time in UTC.

3.2 Detection of recirculation zones

We develop [an algorithm a method](#) to identify recirculation zones in measurements taken by lidars along the measurement transects ([Figure 5](#)). This method is based on measurements by two lidars located on the same transect. By using two lidars, the area covered by the scans within the valley can be maximized. The RHI scans provide [line-of-sight \(LOS\) LOS](#) wind speed measurements in a polar coordinate system with the lidar at the origin. Consequently, two lidars which are measuring in the same vertical plane will provide data in polar coordinate systems with different origins. Therefore, the LOS wind speeds measured by the lidars are interpolated to a Cartesian coordinate system with the abscissa orientated along the [measurement](#) transect and a grid size of 10 m in both the vertical and horizontal directions. In overlap regions, only measurements of the lidar

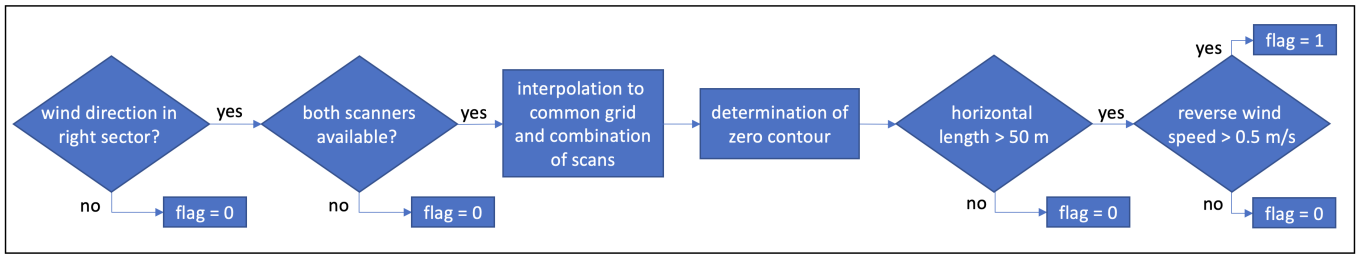


Figure 5. Flow diagram of recirculation zone detection process. Recirculation is detected for periods that are flagged with "1", no recirculation is detected for periods flagged with "0".

further downwind are used. Additional regions that are sampled by the second lidar upwind are filled in a second step. This procedure prevents discontinuities between the two scans from interfering with estimates of the recirculation (figure within the recirculation zone (Figure 4a). Since the elevation angles are small and the procedure in complex terrain is ambiguous, we do not attempt to divide the LOS speeds with the cosine of the beam elevation angle combine LOS velocities measured by the

5 lidars to get the true horizontal wind along the measurement transect, since the elevations angles are too small to measure the vertical component precisely. Moreover, the assumption of zero vertical wind speed, as often applied in flat terrain.

Having the measurements combined, the zero contour line of the velocity field behind the upwind ridge is determined using linear interpolation. The area bounded by this contour and the terrain beneath describes the dimensions of the recirculation zone (figure Figure 4). Recirculation is defined to be presented for reverse flow speeds greater than 0.5 m s^{-1} , which is the measurement accuracy of the lidars (Leosphere, 2016). Also, the length of these zones is required to exceed five grid cells or 10 50 m in the horizontal dimension. To increase the robustness of this method we require that at least one valid measurement is available below the contour line. A potential disadvantage is that recirculation appearing close to the ground cannot be captured since measurement range gates of the lidars that reach into the ground or vegetation must be discarded due to the hard target returns.

15 4 Results and Discussion

The algorithm method to detect the recirculation zones is applied to all available periods so that we can analyze the occurrences of recirculation under different atmospheric conditions in combination with the mast measurements. Specifically, we assess the impact of flow direction, mean flow speed and atmospheric stability. The measurement period from April to mid of June was generally very hot with maximum temperatures above 40°C . Days were normally cloud-free while on some mornings fog 20 formed inside the valley. Therefore, stably stratified atmospheric conditions at night and unstable conditions during the day are prevailing.

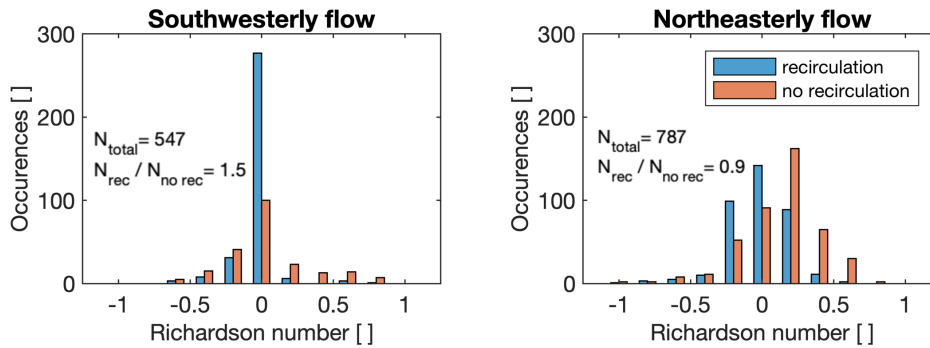


Figure 6. Recirculation occurrence as a function of the Richardson number. The results are presented in bins with a width of 0.2. Data from all three transects are presented together, segregated by the wind direction.

4.1 Occurrence of recirculation

On average, recirculation occurs frequently, in 52% of all 10-min time periods examined. This ratio changes for the individual transects. Along transect 1 (the furthest northwest, with the lowest point in the valley and the shortest distance between ridges), recirculation occurs most frequently at 69% of the time, while transect 2 observes recirculation 51% of the time. Transect 3 (the furthest southeast, with the highest low point in the valley and the longest peak-to-peak distance) only observes recirculation in 32% of the available periods. These variations of recirculation occurrence may be related to the transects' elevation profiles within the valley. The average elevation along transect 1 and 2 is the same, whereas the average elevation along transect 3 is 15 m higher (table Table 2). Additionally, the elevation profile of transect 3 shows a hill at the center of the valley (figure 2 Figure 2). We infer assume that these features suppress the formation of recirculation along transect 3. Other terrain parameters and land use/land cover characteristics only vary insignificantly among the transects.

4.1.1 Dependence on atmospheric stability

Recirculation is more likely to occur during unstable or neutral atmospheric conditions ($Ri \leq 0$) than for stable conditions ($Ri > 0$) for both SW and NE winds (Figure 6), as expect for flow over steep geometries such as the Perdigão ridges. These results resonate with the findings of Kutter et al. (2017), who found, in a study of recirculation at a single forested hill, that recirculation is less likely to occur under stable conditions. In fact, they found only one period with recirculation during stable conditions, whereas we have several such cases of recirculation under stable conditions.

Only the bin centered at $Ri = -0.2$ shows an opposite dominance of recirculation versus no recirculation for the two flow directions. Recirculation occurs in this bin mainly for northeasterly flow (figure Figure 6b), whereas the opposite is true for southwesterly flow (figure Figure 6a). For stability calculations, only measurements from the mast on the northeast ridge are

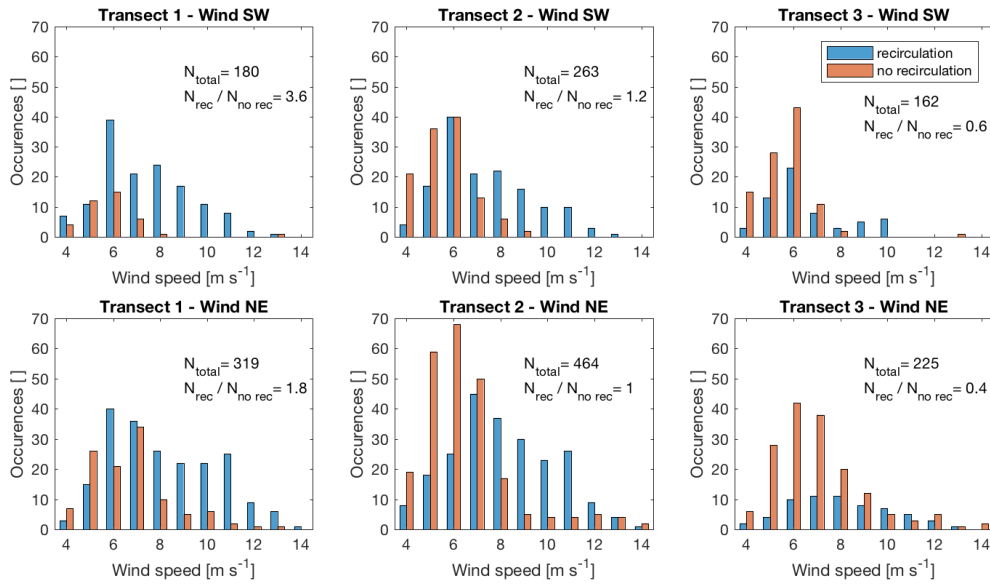


Figure 7. Occurrence of recirculation depending on the mean wind speed measured by the 100 m sonic on the upstream mast. The histograms are separated by transect and wind direction.

used since the availability of temperature measurements at the other mast is very low. Thus, turbulent mixing is increased at the mast location for southwesterly flow which could affect the Richardson number and thereby these results.

4.1.2 Dependence on mean wind direction

Recirculation occurs more often for southwesterly wind directions (figure 7 and 8). A possible explanation for this difference could be the larger height of the southwest ridge, which makes it more likely for recirculation to form. Flow separation and thus flow recirculation is general more likely for increasing heights of obstacles. Moreover, the southwest face of the southwest ridge (the upwind-downwind face in southwesterly flow) is steeper in comparison to the northeast face of the southwest ridge (the upwind-downwind face in northeasterly flow). The average slope at the three transects over 500 m from the peak are 23° at the southwest ridge and 17.6° at the northeast ridge. Strong differences again emerge among the transects (figure 8). Both, the higher steepness and the escarpments, make flow separation more likely. At transect 1 recirculation occurs predominantly, especially for southwesterly flow. The ratio of periods with recirculation occurrence to no occurrence is balanced at transect 2, and at transect 3 recirculation can only be observed 32% of the time. For all transects the chance of recirculation is higher for southwesterly wind directions.

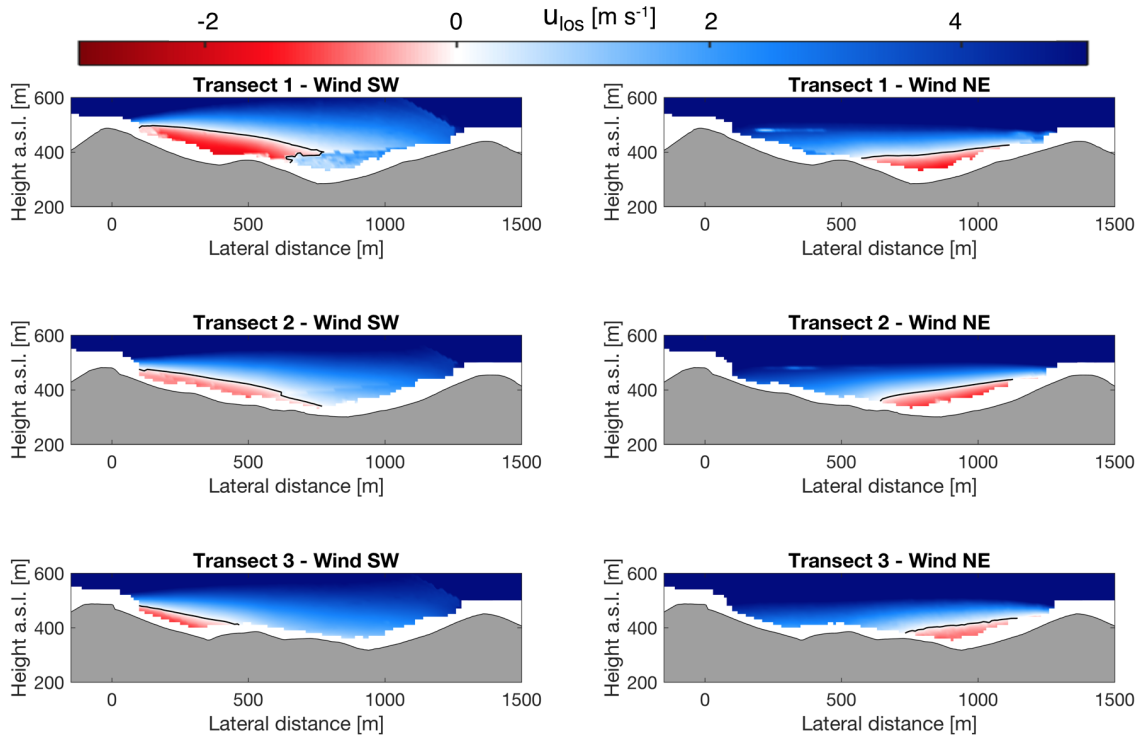


Figure 8. Zero contour line (black line) defining the upper border of recirculation zones of the mean velocity field of all recirculation periods per transect and flow direction. The flow speed is positive in the direction of the mean flow field and the transect origins (lateral distance = 0) refers to the position of the WindScanner 105, 102 and 106 for transect 1, 2, and 3, respectively.

4.1.3 Dependence on mean wind speed

More differences between the transects emerge when we group the data by wind speed. Transects 1 and 2 show a very high chance of recirculation to occur for wind speeds above 8 m s^{-1} (figure Figure 7). For wind speeds above 8 m s^{-1} , fewer cases of recirculation occur for northeasterly wind directions, whereas recirculation is present in almost all cases for southwesterly wind directions. Moreover, the wind speed bin of 6 m s^{-1} shows interesting results in the inter-transect comparisons: at transect 1, recirculation dominates this bin, whereas a contrary trend can be observed at the other transects.

4.1.4 Characteristics under stratified conditions

The findings above show that recirculation occurs as expected prevailingly under unstable atmospheric conditions but occurrences under stably stratified conditions are not absent. In general, three types of behaviours can be expected when flow encounters an obstacle (e.g. a hill or a ridge), (i) complete attachment of the flow, separation downstream is suppressed by strong stratification; (ii) downstream separation of flow direction directly behind the obstacle; and (iii) post-wave separation (Baines, 1998). The

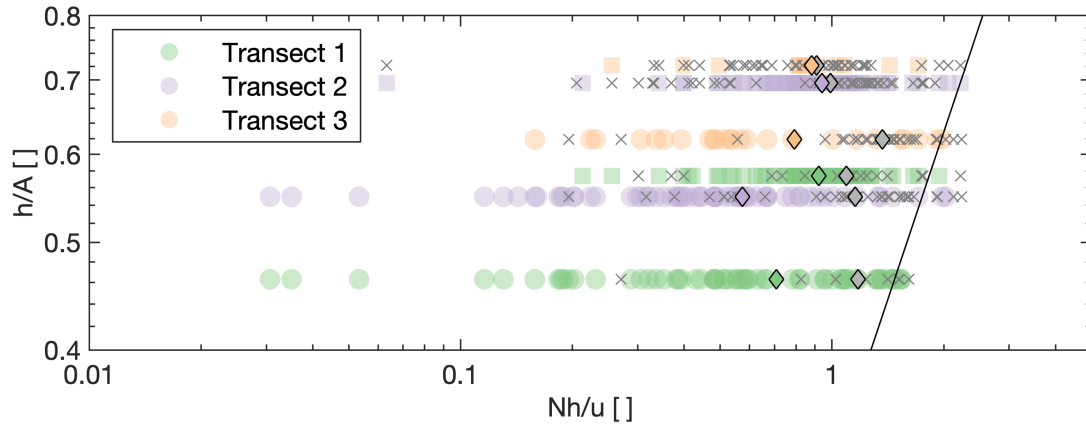


Figure 9. Observational periods with recirculation (colored markers) and without recirculation (gray cross marks) under stratified conditions as a function of mean lee-side slope (h/A) and Nh/u . The round markers refer to recirculation at the southwest ridge and the square markers to northeast ridge. The colored diamond markers show the mean value of Nh/u per transect during periods with recirculation and the gray markers the mean for periods without recirculation. The solid black line shows where $NA/u = \pi$.

occurrence of these behaviours is sensitive to the downstream slope h/A of the obstacle and Nh/u . Steeper downstream slopes support the formation of flow separation behind an obstacle and stronger stratification and higher values (separation occurs when $NA/u < \pi$) of Nh/u suppress separation respectively. The relation of these mechanisms is well summarized in Figure 5.8 in Baines (1998) and we present our findings in the same non-dimensional framework in Figure 9. The observations made in Perdigão, recirculation and non recirculation periods, are falling almost entirely in an area where $NA/u < \pi$ in which separation is expected. However, looking at the mean value for recirculation and non recirculation periods it becomes noticeable that the mean of non recirculation periods of Nh/u is higher consistently at all transects. The higher mean value of non recirculation periods aligns with the expectations described above to find attached flow or post-wave separation (which is not necessarily detected by our detection method) for higher values of Nh/u .

10 4.2 Recirculation zone characteristics

The observed recirculation zones can be described by their shape in terms of extent and height and the magnitude of reverse flow speed. On average, the observed recirculation areas extend to 697 m in the horizontal for both wind directions, which is almost exactly half the average ridge-to-ridge distance at the transects. At the southeastern transect (transect 3, the longest transect with the least frequent recirculation), the average extent is 22% smaller than the mean of all transects (figure 7 Figure 4). The average extent at the northwestern transect (transect 1, the shortest transect), is 9% higher than the average extent. The average depth of observed recirculation zones is 157 m above the valley bottom height and changes insignificantly among the transects, whereas the maximum depth shows larger variation among the transects. We found that recirculation zones at transect 1 reach up to 300 m above the valley bottom and 215 m and 189 m at transect 2 and 3, respectively. Maximum reverse

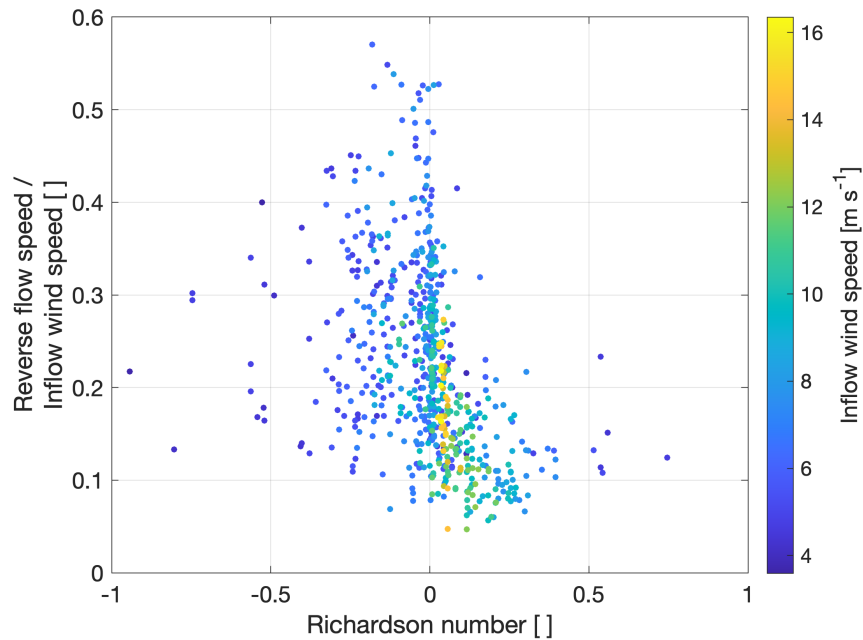


Figure 10. Reverse flow speed as a function of divided by the inflow wind speed over the Richardson number. The color scaling shows the wind speed measured at the upstream mast 100 m above ground. Data points are colored according to the Richardson number.

flow speeds of above 4 m s^{-1} are observed. The median reverse flow speeds at the transects are 2.0 , 1.5 and 1.4 m s^{-1} for transect 1, 2 and 3, respectively. For all transects and both flow directions combined, a trend for higher reverse flow speeds for Richardson numbers close to zero is found (figure Figure 10). For Richardson numbers greater than 0.5 and smaller than -0.5 all transects and both flow directions combined the relation of the reverse flow speeds are in most cases below 2 m s^{-1} . The to

5 the Richardson number is presented in Figure 10. The reverse flow speed measurements are divided by the inflow wind speed limits the maximum reverse flow speed for wind speeds below 6 m s^{-1} , and from the measured at the meteorological masts. For unstable atmospheric conditions ($Ri < 0$) no clear trend for the relation of reverse wind speed and inflow wind speed can be observed. Ratios from less than 0.1 to more than 0.5 can be observed. During conditions with $Ri > 0$ ratios are generally lower and appear to decrease with increasing Ri . For high wind speeds (greater than 12 m s^{-1} the average observed reverse speed

10 increases) ratios of less than 0.3 are observed and they occur, as expected, for small or slightly positive Richardson numbers.

4.3 Impact on potential turbine sites

Ridges and hills are advantageous sites for wind turbines, due to the terrain-induced speed-up (Hunt and Snyder, 1980). However, these stronger winds can come at a cost, due to higher turbulence levels and gustiness which increases loads and

Table 3. Comparison of wind characteristics during the period 2017/05/05 16:30 - 16:40 UTC measured by the sonic anemometers at 100-m height on the upwind southwest (SW) and downwind northeast (NE) ridges. Turbulence intensity is defined as $I = \sigma_U \bar{U}^{-1}$ where \bar{U} is the mean wind speed and σ_U the standard deviation of U . Turbulent kinetic energy is calculated as $e = \frac{1}{2} [\overline{u'^2} + \overline{v'^2} + \overline{w'^2}]$, where u' , v' and w' are the fluctuating parts of the wind vector components over a 10-min average as measured by the sonic anemometers.

	SW ridge (100m)	NE ridge (100m)
Wind speed, \bar{U} [m s^{-1}]	10.4	5.2
Wind direction [$^\circ$]	254.1	239.7
Turbulence intensity, I [%]	11.8	30.7
Turbulent kinetic energy, e [$\text{m}^2 \text{s}^{-2}$]	2.26	4.32
Wind veer (60-100 m) [$^\circ$]	-2.1	-13.7

decreases the lifetime of turbines. In this section, we assess differences in wind characteristics at the downwind ridge for both the entire dataset as well as a specific case study of the period shown in [figure Figure 4](#).

4.3.1 Case study of recirculation under neutral stratification

On May 5 from 16:30 to 16:40 UTC, winds were 10.4 m s^{-1} from the southwesterly direction (254°). A strong and distinct recirculation zone occurred behind the southwest ridge within the valley at the second transect ([figure Figure 4](#)). The zone has a total length of 807 m, spreading out beyond the valley center. It reaches over the ridge-peak height to 192 m above the valley bottom. Reverse flows inside the recirculation zone have a magnitude of up to 1.8 m s^{-1} , or 17% of the inflow.

~~The recirculation zone also influences flow at the northeast ridge. The leeward recirculation zone and terrain wake of the southwest ridge decrease the~~ For this case with a strong recirculation zone we observe a reduction in mean wind speed and increase the turbulence intensity further downwind at the northeast ridge. Measurements at the meteorological masts show the impact at the downwind ridge ([table Table 3](#)). At the 100-m level, the wind speed is reduced 50% as compared to the upwind 100-m mast. Similarly, the turbulence intensity increases from 12% at the upwind ridge to 31% at the downwind ridge. The wind veer observed from 60 to 100 m equals 14° at the downwind ridge versus 2° at the upwind. Moreover, the lidar scan shows that the wake of the upwind ridge reaches to approximately 250 m above the northeast peak height ([figure Figure 4](#)).

4.3.2 General impact of recirculation at downwind locations

The detailed analysis of the period in the previous section shows significant changes of the wind characteristics at the downwind ridge. To generalize this observation, we analyze all periods available from transect 2 (on which the measurement masts are located), or 455 (260) periods to consider for northeasterly (southwesterly) flow. The measurements of 10-minute mean wind speed U (we drop the bar for simplicity) ~~and turbulence intensity I~~ at the downwind ridge are normalized for each period by

Table 4. Changes in the wind characteristics at the downwind ridge.

	SW wind direction		NE wind direction	
	recirculation	no recirculation	recirculation	no recirculation
$\overline{I_{upwind}}$ [%]	13.0	13.5	11.2	8.4
$\overline{I_{downwind}}$ [%]	20.8	16.6	13.1	9.2
$\overline{\Delta U}$ [%]	-7.1	2.5	15.5	19.3
N [-]	142	118	225	230

dividing with the measurements taken at the upstream ridge:

$$\Delta(U) = \frac{\text{median}(U_{downwind})}{\text{median}(U_{upwind})} \frac{(U_{downwind} - U_{upwind})}{U_{upwind}} \cdot 100; \quad \Delta(I) = \frac{\text{median}(I_{downwind})}{\text{median}(I_{upwind})} \quad (3)$$

At both ridges, data from the 100-m sonic anemometers are used. For both wind directions, a decrease in mean wind speed and an increase in turbulence intensity when recirculation is present is found at the downwind ridge (table-Table 4). For southwesterly wind directions which tended to have larger and more vigorous recirculation zones, these changes are more pronounced. Notice, the median-mean of I for recirculation periods, normalized with the median of non-recirculation periods, shows a proportional increase of I at the downwind ridge of 34.5% (13.9 compared to upwind ridge of 7.8% (1.9%)) for southwesterly (northeasterly) wind directions. During periods without recirculation I only increases by 3.1% (0.8%) for southwesterly (northeasterly) wind directions.

10 5 Conclusions

Recirculation zones at two parallel ridges have been analyzed using line-of-sight measurements from six long-range WindScanners and two 100-m measurement masts equipped with sonic anemometers. The data were collected during the Perdigo 2017 measurement campaign in spring and summer 2017 in central Portugal. Algorithms are An method is developed to detect recirculation zones from RHI scans performed at three transects perpendicular to the ridges. Atmospheric stability is characterized using measurements of sonic anemometers and temperature sensors on a 100-m mast on the ridges.

For flow perpendicular to the ridges, recirculation occurs frequently, in 52% of the scans, 55% for southwesterly wind and 49% for northeasterly. The occurrence of recirculation depends on mean wind speed and atmospheric stability. Recirculation is more likely for wind speeds above 8 m s^{-1} (measured 100 m above the ridges) and is less likely during stable atmospheric conditions.

20 An inter-comparison of the recirculation occurrence per transect revealed significant differences. The northwestern transect shows a 69% probability of recirculation to occur, compared to a 32% probability at the southeastern-most transect, perhaps due to the topographic variations between the transects.

Finally, recirculation affects the wind characteristics which are of importance for wind energy generation at the downwind ridge. During recirculation periods, the mean wind speed is lower at the downwind ridge than when recirculation is not present. Further, turbulence intensity is increased at the downwind ridge. These increases in turbulence intensity were not symmetric: a ~~proportional~~ increase of the ~~median-mean~~ turbulence intensity of ~~34.5%~~ ~~(13.97.8%~~ (3.1%) is found at the downwind ridge
5 for southwesterly (northeasterly) flow compared to the upwind ridge. These differences can result from differences in the orography: slopes at the southwest ridge are steeper compared to the northeast ridge and the southwest ridge is higher than the northeast ridge. These findings are of importance for wind energy projects in complex terrain. Developers may reduce loads on turbines, and thereby increase turbine lifetimes, by considering the spatial extent of recirculation zones and positioning the turbines accordingly. Because assessment with multiple scanning lidars, as presented in this study, is yet not feasible for
10 commercial projects, efforts should be ~~make-made~~ to account for recirculation in the flow models used for wind resource assessment.

Data availability. All data sets measured during the Perdigão 2017 campaign are publicly available through dedicated web portals of the University of Porto (<https://windsp.fe.up.pt/>) and NCAR/EOL (http://data.eol.ucar.edu/master_list/?project=PERDIGAO). The lidar dataset measured by DTU is additionally available under the following DOI: <https://doi.org/10.11583/DTU.7228544.v1>

Author contributions. R. Menke performed the analysis and wrote the main body of the manuscript. J. K. Lundquist, J. Mann and N. Vasiljević gave scientific advice. R. Menke, J. Mann and N. Vasiljević designed the lidar part of the field campaign. All authors contributed with critical feedback to this manuscript.

Competing interests. The authors declare that they have no conflict of interest.

Acknowledgements. We acknowledge the work of everyone involved in the planning and execution of the campaign, in specific we would like to thank Stephan Voß, Julian Hieronimus (ForWind, University of Oldenburg), Per Hansen and Preben Aagaard (DTU Wind Energy) for their help with the installation of the WindScanners and Steven Oncley and Kurt Knudson (National Center for Atmospheric Research) for their help with the installation of the meteorological [towersmasts](#). We are also grateful for the contribution of three WindScanners to the campaign by ForWind. Moreover, only the intensive negotiations of José Carlos Matos, INEGI with local landowners about specific locations for our WindScanners made this research possible. We are grateful to the municipality of Vila Velha de Ródão, landowners who authorized installation of scientific equipment in their properties, the residents of Vale do Cobreão, Foz do Cobreão, Alvaiade, Chão das Servas and local businesses who kindly contributed to the success of the campaign. The space for operational centre was generously provided by Centro Sócio- Cultural e Recreativo de Alvaiade in Vila Velha de Rodão. We thank the Danish Energy Agency for funding through the New European Wind Atlas project (EUDP 14-II). J. K. Lundquist's effort is supported by the U. S. National Science Foundation under grant AGS-1565498.

References

- Aitken, M. L., Banta, R. M., Pichugina, Y. L., and Lundquist, J. K.: Quantifying Wind Turbine Wake Characteristics from Scanning Remote Sensor Data, *Journal of Atmospheric and Oceanic Technology*, 31, 765–787, <https://doi.org/10.1175/JTECH-D-13-00104.1>, 2014.
- Baines, P.: *Topographic Effects in Stratified Flows*, Cambridge Monographs on Mechanics and Applied Mathematics, Cambridge University Press, 1998.
- Burns, S. P., Sun, J., Lenschow, D. H., Oncley, S. P., Stephens, B. B., Yi, C., Anderson, D. E., Hu, J., and Monson, R. K.: Atmospheric Stability Effects on Wind Fields and Scalar Mixing Within and Just Above a Subalpine Forest in Sloping Terrain, *Boundary-Layer Meteorology*, 138, 231–262, <https://doi.org/10.1007/s10546-010-9560-6>, 2011.
- Chow, F. K. and Street, R. L.: Evaluation of Turbulence Closure Models for Large-Eddy Simulation over Complex Terrain: Flow over Askervein Hill, *Journal of Applied Meteorology and Climatology*, 48, 1050–1065, <https://doi.org/10.1175/2008JAMC1862.1>, 2009.
- Fernando, H., Mann, J., Palma, J., Lundquist, J., Barthelmie, R., BeloPereira, M., Brown, W., Chow, F., Gerz, T., Hocut, C., Klein, P., Leo, L., Matos, J., Oncley, S., Pryor, S., Bariteau, L., Bell, T., Bodini, N., Carney, M., Courtney, M., Creegan, E., Dimitrova, R., Gomes, S., Hagen, M., Hyde, J., Kigle, S., Krishnamurthy, R., Lopes, J., Mazzaro, L., Neher, J., Menke, R., Murphy, P., Oswald, L., Otarola-Bustos, S., Pattantyus, A., Rodrigues, C. V., Schady, A., Sirin, N., Spuler, S., Svensson, E., Tomaszewski, J., Turner, D., van Veen, L., Vasiljević, N., Vassallo, D., Voss, S., Wildmann, N., and Wang, Y.: The Perdigão: Peering into Microscale Details of Mountain Winds, *Bulletin of the American Meteorological Society*, <https://doi.org/10.1175/BAMS-D-17-0227.1>, 2018.
- Finnigan, J. and Belcher, S.: Flow over a hill covered with a plant canopy, *Quarterly Journal of the Royal Meteorological Society*, 130, 1–29, 2004.
- Hunt, J. C. R. and Snyder, W. H.: Experiments on stably and neutrally stratified flow over a model three-dimensional hill, *Journal of Fluid Mechanics*, 96, 671, <https://doi.org/10.1017/S0022112080002303>, 1980.
- Iungo, G. V., Wu, Y.-T., and Porté-Agel, F.: Field Measurements of Wind Turbine Wakes with Lidars, *Journal of Atmospheric and Oceanic Technology*, 30, 274–287, <https://doi.org/10.1175/JTECH-D-12-00051.1>, 2013.
- Kaimal, J. C. and Finnigan, J. J.: *Atmospheric boundary layer flows: their structure and measurement*, Oxford university press, 1994.
- Kutter, E., Yi, C., Hendrey, G., Liu, H., Eaton, T., and Ni-Meister, W.: Recirculation over complex terrain: Recirculation Over Complex Terrain, *Journal of Geophysical Research: Atmospheres*, 122, 6637–6651, <https://doi.org/10.1002/2016JD026409>, 2017.
- Käsler, Y., Rahm, S., Simmet, R., and Kühn, M.: Wake Measurements of a Multi-MW Wind Turbine with Coherent Long-Range Pulsed Doppler Wind Lidar, *Journal of Atmospheric and Oceanic Technology*, 27, 1529–1532, <https://doi.org/10.1175/2010JTECHA1483.1>, 2010.
- Lange, J., Mann, J., Angelou, N., Berg, J., Sjöholm, M., and Mikkelsen, T.: Variations of the Wake Height over the Bolund Escarpment Measured by a Scanning Lidar, *Boundary-Layer Meteorology*, 159, 147–159, <https://doi.org/10.1007/s10546-015-0107-8>, 2016.
- Lange, J., Mann, J., Berg, J., Parvu, D., Kilpatrick, R., Costache, A., Chowdhury, J., Siddiqui, K., and Hangan, H.: For wind turbines in complex terrain, the devil is in the detail, *Environmental Research Letters*, 12, 094 020, <https://doi.org/10.1088/1748-9326/aa81db>, 2017.
- Leosphere: Leosphere WindCube 100S/200S/400S brochure, http://www.leosphere.com/wp-content/uploads/2016/12/Brochure-Scanning-Lidar-Weather-and-Climat_BD.pdf, 2016.
- Mann, J., Angelou, N., Arnqvist, J., Callies, D., Cantero, E., Arroyo, R. C., Courtney, M., Cuxart, J., Dellwik, E., Gottschall, J., Ivanell, S., Kühn, P., Lea, G., Matos, J. C., Palma, J. M. L. M., Pauscher, L., Peña, A., Rodrigo, J. S., Söderberg, S., Vasiljevic, N., and Rodrigues,

- C. V.: Complex terrain experiments in the New European Wind Atlas, *Philosophical Transactions of the Royal Society A: Mathematical, Physical and Engineering Sciences*, 375, 20160101, <https://doi.org/10.1098/rsta.2016.0101>, 2017.
- Menke, R., Vasiljevic, N., Hansen, K., Hahmann, A. N., and Mann, J.: Does the wind turbine wake follow the topography? - A multi-lidar study in complex terrain, *Wind Energy Science*, p. 18, 2018.
- 5 Rotach, M. W. and Zardi, D.: On the boundary-layer structure over highly complex terrain: Key findings from MAP, *Quarterly Journal of the Royal Meteorological Society*, 133, 937–948, <https://doi.org/10.1002/qj.71>, 2007.
- Sathe, A., Mann, J., Barlas, T., Bierbooms, W., and van Bussel, G.: Influence of atmospheric stability on wind turbine loads: Atmospheric stability and loads, *Wind Energy*, 16, 1013–1032, <https://doi.org/10.1002/we.1528>, 2013.
- Silva Lopes, A., Palma, J. M. L. M., and Castro, F. A.: Simulation of the Askervein flow. Part 2: Large-eddy simulations, *Boundary-Layer Meteorology*, 125, 85–108, <https://doi.org/10.1007/s10546-007-9195-4>, 2007.
- 10 Sogachev, A., Rannik, Ü., and Vesala, T.: Flux footprints over complex terrain covered by heterogeneous forest, *Agricultural and Forest Meteorology*, 127, 143–158, <https://doi.org/10.1016/j.agrformet.2004.07.010>, 2004.
- Stull, R. B.: *An Introduction to Boundary Layer Meteorology*, Springer Science & Business Media, 2012.
- Taylor, P. A. and Teunissen, H. W.: Askervein'82: Report on the September/October 1982 Experiment to Study Boundary Layer Flow over
- 15 Askervein, South Uist, Meteorological Services Research Branch, Atmospheric Environment Service, 1983.
- Troen, I. and Petersen, E. L.: *European wind atlas*, Published for the Commission of the European Communities, Directorate-General for Science, Research, and Development, Brussels, Belgium by Risø National Laboratory, Roskilde, Denmark, 1989.
- Vasiljevic, N., Lea, G., Courtney, M., Cariou, J.-P., Mann, J., and Mikkelsen, T.: Long-range WindScanner system, remote sensing, p. 26, 2016.
- 20 Vasiljević, N., Palma, J. M. L. M., Angelou, N., Matos, J. C., Menke, R., Lea, G., Mann, J., Courtney, M., Ribeiro, L. F., and Gomes, V. M. M. G. C.: Perdigoão 2015: methodology for atmospheric multi-Doppler lidar experiments, *Atmospheric Measurement Techniques*, pp. 1–28, <https://doi.org/10.5194/amt-2017-18>, 2017.
- WASP: Wind Atlas Analysis and Application Program, last accessed: January 31, 2019, <http://www.wasp.dk>.
- Wood, N.: The onset of separation in neutral, turbulent flow over hills, *Boundary-Layer Meteorology*, 76, 137–164,
- 25 <https://doi.org/10.1007/BF00710894>, 1995.
- Xu, X. and Yi, C.: The influence of geometry on recirculation and CO₂ transport over forested hills, *Meteorology and Atmospheric Physics*, 119, 187–196, <https://doi.org/10.1007/s00703-012-0224-6>, 2013.